CONF-830607--27

## DISCLAIMER



# FATIGUE OF LMFBR PIPING DUE TO FLOW STRATIFICATION

W. S. WOODWARD
Senior Engineer
Member ASME
Westinghouse Electric Corp.
Madison, PA

CONF-830607--27

DE84 001851



ABSTRACT

Flow stratification due to reverse flow was simulated in a 1/5 scale water model of a LMFBR primary pipe loop. The stratified flow was observed to have a dynamic interface region which oscillated in a wave pattern. The behavior of the interface was characterized in terms of location, local temperature fluctuation and duration for various reverse flow conditions. A structural assessment was performed to determine the effects of stratified flow on the fatigue life of the pipe. Both the static and dynamic aspects of flow stratification were examined. The dynamic interface produces thermal striping on the inside of the pipe wall which is shown to have the most deleterious effect on the pipe wall and produce significant fatigue damage relative to a static interface.

INTRODUCTION

Flow stratification is a phenomenon which has the potential to cause significant fatigue damage in liquid metal pipe systems. Stratified flow can occur in loop type LMFBR primary pipe systems during remote events which involve both a pony motor failure in one loop and check valve leakage. During these events reverse flow may initiate in the affected loop and cold sodium residing in the intermediate heat exchanger (IHX) is pushed backwards out of the inlet nozzle and up through the hot leg pipe. Flow stratification may develop when the cold sodium reaches a horizontal pipe section containing hot sodium. The controlling parameter for identifying the initation of flow stratification is the dimensionless Richardson number. The Richardson number represents the ratio of bouyancy forces to the inertial forces in the fluid flow. The bouyancy forces are due to the difference in density between the hot and cold fluids and under low velocity reverse flow conditions the bouyancy forces dominate the inertial forces and stratification develops. The interface region between the hot and cold sodium layers is of particular interest because large variations in local fluid temperature coupled with characteristically high film coefficients can produce large variations in temperature in the pipe wall. The resulting thermal stress fluctuations contribute to fatigue of the pipe.

Until recently there has been little research directed toward the understanding of flow stratification in piping systems. The fluid phenomenon is currently being evaluated by Kasza at Argonne National Laboratory for piping systems prototypic of those found in loop type LMFBRs. This test program is intended to give pipe designers an understanding of the problem and provide recommendations on how to minimize stratification

NOMENCLATURE

| | | | |
|---|---|---|---|
| $b$ | Thickness of pipe wall | $\alpha$ | Thermal diffusivity |
| $D$ | Inside diameter of a pipe | $\beta$ | Dimensionless thickness, $\sqrt{w/2\alpha}b$ |
| $D_h$ | Hydraulic diameter = 4·(Flow area)/(Wetted perimeter) | $\varepsilon$ | Strain |
| | | $\Delta\rho$ | Difference in density due to temperature difference $\Delta T$ |
| $E$ | Young's modulus | $\Delta T$ | Maximum temperature difference in fluid |
| $g$ | Gravitation acceleration | $\delta$ | Surface to average temperature difference |
| $h$ | Film coefficient | $\eta$ | $\Delta T$ surface/$\Delta T$ fluid |
| $k$ | Thermal conductivity | $\theta_m$ | Angle from vertical indicating location of central position of the stratified interface |
| $R_i$ | Inside radius of pipe | | |
| $R_o$ | Outside radius of pipe | $\rho$ | Density |
| $t$ | Thickness of interface region | $\omega$ | Frequency of oscillation |
| $V$ | Flow velocity | | |

effects. Kasza has developed a correlation between the Richardson number and the initiation of flow stratification. These results indicate that stratification will probably develop during low velocity reverse flow events in LMFBR primary pipe systems. Fujimoto [1] performed tests to investigate flow stratification in pipes with the specific purpose of studying the fluid behavior in the vicinity of the interface between the hot and cold fluids. He observed significant wave motion at the interface which resembled the wave motion of flow in an open channel. Moreover, he concluded that the film coefficients at the interface were as high as seven times nominal values. Although these studies provide key data in quantifying the fluid phenomenon, they do not address the effects of stratification on the pipe structure.

The purpose of the present study is to provide an understanding of how flow stratification contributes to fatigue damage in LMFBR primary pipe systems. Stratified flow was simulated for reverse flow conditions in a series of scaled water tests. The fluid behavior was observed and local fluid temperature fluctuations were measured. Under reverse flow conditions, highly dynamic thermal fluctuations were observed which were due to the wave motions of the interface of the hot and cold fluid layers. In this study, fatigue damage due to static stratified flow and the dynamic wave motions are examined. It is demonstrated that the dynamic nature of stratification can be the most deleterious to the pipe wall.

## WATER MODEL TESTS

Reverse flow events, typical of those which occur in loop type LMFBR primary pipe systems, were simulated in scaled water model tests. The objective is to obtain fluid temperatures for use in calculating pipe wall temperatures and subsequently thermal stresses and fatigue damage. The model was constructed from plexiglass pipe and is illustrated in Figure 1. The model includes a large diameter (6.5 inch I.D.) hot leg which connects the reactor vessel with the primary pump and a smaller diameter (4.0 inch I.D.) hot leg connecting the primary pump and intermediate heat exchanger (IHX). The volume of fluid in the pump model is representative of the volume of fluid in a scaled primary pump, however, the pump dynamics were not modeled. The pipe model was initially filled with static 130°F water. Reverse flow was simulated by injecting 70°F water at the IHX inlet. Dye was injected into the cold stream for flow visualization. Transient fluid temperature were measured at cross sections 1 through 5 (Figure 1) using closely spaced thermocouples around the circumference of the pipe wall. The thermocouples were Type K grounded thermocouples with time constants in a range of 0.1 - 0.3 seconds. Figure 2 illustrates the placement of thermocouples in the cross sections. This arrangement was designed specifically to detect the location of the interface between the hot and cold layers as stratified flow developes and moves up through the cross section.

### Test Conditions

The selection of parameters for the scaled water tests was based on similitude of the Richardson number

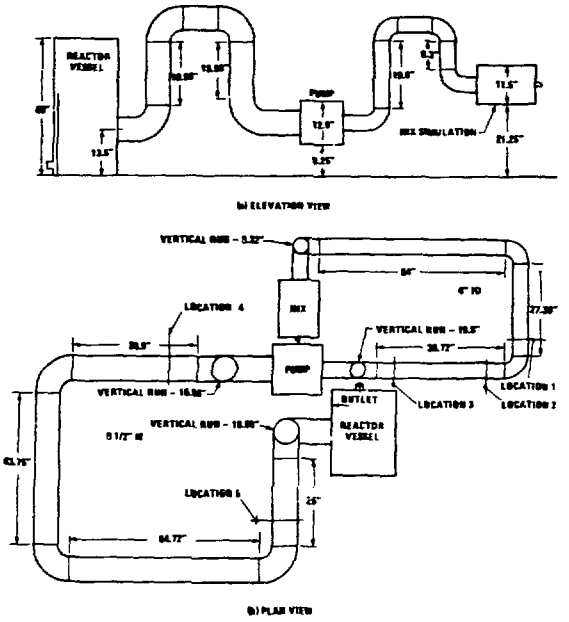


Figure 1 Water Model of a LMFBR Primary Hot Leg

$$Ri = \frac{\Delta\rho}{\rho}\,\frac{gD}{V^2} \qquad (1)$$

Reverse flow velocities were selected such that Richardson numbers in the tests were equal to prototypic values for a LMFBR primary pipe system. Maximum reverse flows in current LMFBR designs are limited by check valve leakage to 1100 GPM. The maximum difference in sodium temperature for reverse flow events in loop type LMFBRs is 400°F. Diameters of 23 inches and 35 inches were used as diameters for prototypic hot leg pipes and Richardson numbers were calculated for maximum reverse flow velocities in each pipe leg. Test flow rates were based on simulation of 42 percent to 100 percent of the maximum reverse flow rates. The selected test conditions are summarized in Table 1.

Establishing similitude based on the Richardson number does not insure complete similitude between the model and prototype. The Reynolds numbers should be equivalent for dynamic similitude and the Prandtl numbers should be equivalent for thermal similitude. For these tests similitude of both the Reynolds number and Prandtl number cannot be established concurrently with the similitude of the Richardson number. The Reynolds numbers of the reverse flow for actual plant events are turbulent being in a range of $10^5$-$10^6$. The Reynolds numbers in the tests fall in the laminar to turbulent transition range (Table 1). Thus, the dynamics of the fluid in the test do not simulate that of the plant. Although similitude in dynamics is not rigoriously established, tests which have turbulent flow regimes should provide reasonable dynamic simulation. Moreover, the thermal

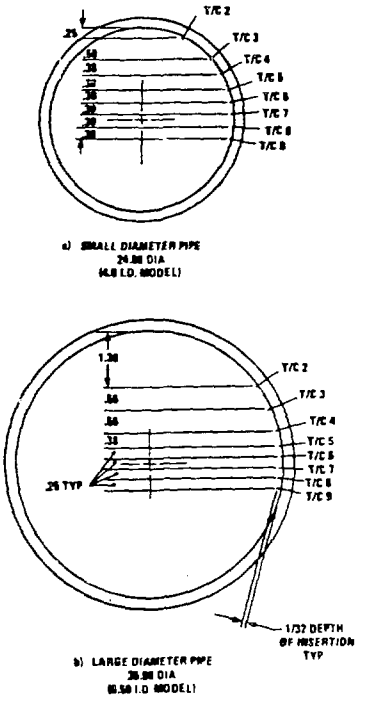


Figure 2 Location of Thermocouples in Pipe Cross Sections

gradients in actual plant events are expected to be much lower than in the tests because the Prandtl number of sodium is of the order of 1000 times lower than that of water. The effect of Prandtl number is judged to dominate over any differences in dynamic behavior between the test and the plant. Thus, thermal gradients observed in the water tests will be greater than those in a LMFBR primary pipe system and thermal stresses calculated from the water test data will be conservative.

## Observations and Results

Stratification was observed to develop under all test conditions. The interface between the hot and cold fluids moved slowly up through the cross sections until the entire pipe was filled with cold fluid. Based on the duration and the amplitude of fluid temperature difference, the worst locations in the small and large pipe sections were 2 and 5 respectively. Figure 3 illustrates the temperature distribution at location 2. The time required to completely wash out the hot fluid increased with increasing Richardson number. Illustrating this point, stratification disappeared after 500 seconds at location 2 for a flow rate of 6.0 GPM while it persisted after 4000 seconds at location 5 with a flow rate of 3.0 GPM. The thickness of the interface region, within which the temperature changed from the hot fluid temperature to that of the cold fluid, varied in the range of 0.6 to 2 inches.

TABLE 1

SUMMARY OF TEST CONDITIONS

| Pipe Section | Cold Water Flow Rate (GPM) | Ri | $Re^*_3$ x10 |
|---|---|---|---|
| 4.0 inch I.D. | 6.0 | 5.3 | 8.5 |
| | 4.5 | 9.5 | 6.4 |
| | 3.0 | 21.4 | 4.3 |
| 6.5 inch I.D. | 7.1 | 44.0 | 6.1 |
| | 5.0 | 88.0 | 4.3 |
| | 3.0 | 244 | 2.3 |

* $Re = \frac{VD_h}{\nu}$, V and $D_h$ are based on reverse flow through bottom half of pipe.

Another significant observation was the oscillation of the interface region. Forces in the shear flow caused the stratified interface to fluctuate in a wave motion similar to that described by Fujimoto. This was most pronounced at low Richardson numbers. The movement of the interface region causes severe transient thermal fluctuations in the pipe wall termed "thermal striping". Figure 4 illustrates the resulting local temperature variation for the worst case thermal striping. Note that the curves in Figure 3 denote average data because local fluctuations such as those shown in Figure 4, are filtered out. The frequency of the thermal striping varies between 0.1 and 0.5 Hertz and under worst case conditions the amplitudes are as high as 60 percent of the maximum difference in fluid temperature. The worst case thermal striping was measured by thermocouple 4 at location 2 during the 4.5 GPM test. The duration of the striping was 440 seconds. A total of 102 cycles was counted. Fifteen percent of this total measured less than ten percent of the fluid $\Delta T$. Seventy percent of the cycles were less than thirty-five percent of the fluid $\Delta T$ while only two percent measured less than sixty percent of the fluid $\Delta T$. Thus only a small percent of the total cycles approached the maximum amplitude.

Thus, two sources of fatigue were identified in these tests. The first source is from stress due to the presence of a static stratified fluid which maintains the top of the pipe at a higher temperature than the bottom. The second source is from stress due to the dynamics of the interface region which produces thermal striping on the pipe wall. The thermal stresses which result from these two phenomena are examined in the next section.

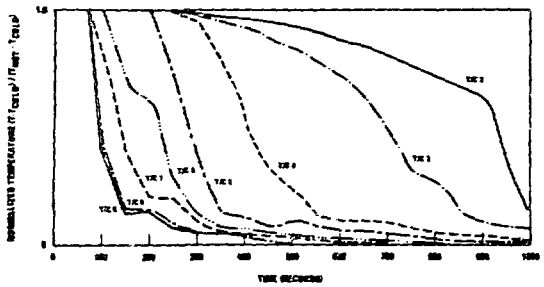

Figure 3 Worst Case Average Temperature Distributions in the Small Diameter Pipe

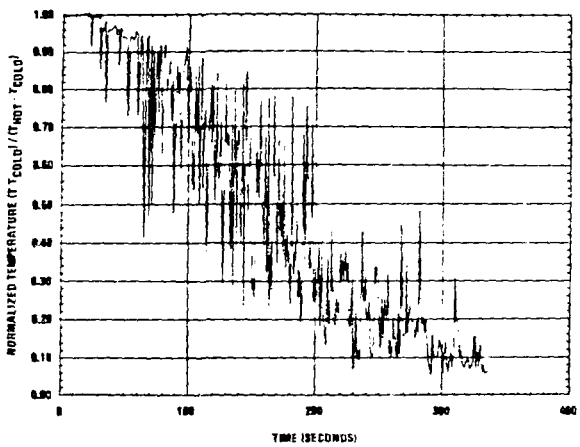


Figure 4 Response of Thermocouple Illustrating Worst Case Thermal Striping Fluctuations

## THERMAL STRESSES

Thermal stresses which result from stratification were studied as a basis for assessing fatigue damage. In order to simplify the analysis, the thermal gradients in the pipe wall were decoupled into two categories based on the two features of stratification previously identified. They are:

A. static stratification represented by hot and cold layers of sodium separated by an interface region and

B. thermal striping due to the oscillation of the interface.

Neglecting oscillation of the interface, the movement of the stratification up through the pipe cross section is sufficiently slow that the assumption of the "static" interface closely approximates the phenomenon. The thermal and stress distributions for this problem are essentially time-independent. In contrast, the oscillation of the interface is relatively fast, producing time-dependent distributions of temperature and stress in the pipe wall. The distributions of temperature and elastic stress for both of these problems are examined in this section.

### Static Flow Stratification

The temperature gradients and stresses due to static stratified flow were assessed using the WECAN finite element program [2]. Finite element models were constructed of 2-D quadratic isoparametric elements and are illustrated in Figure 5. The models represent a large diameter thin walled 316 SS pipe, typical of those found in loop type LMFBRs. The fluid was modeled as an isothermal hot (1000°F) layer of sodium residing over an isothermal cold (600°F) layer of sodium separated by an interface region within which the fluid temperature varied linearly. A parametric study was performed to examine the sensitivity of solutions to variables which are necessarily assumed in the analysis. The parameters varied in the thermal analysis are the interface thickness, t, the film coefficients in each region, h, and the location of the interface $\theta_m$. These variables are illustrated in Figure 6. Linear elastic stress solutions were generated from the resulting thermal distributions and the additional variable of pipe constraint was introduced in the calculation of stress. Internal pressure was neglected.

The values of the variables examined in the parametric study are listed in Table 2. Interface thicknesses span those observed in the water model test. The largest value was judged to be representative of actual in sodium gradients. The heat transfer between the fluid and pipe was modeled while the outside pipe was adiabatic. Bounding values of film coefficients were based on static hot sodium and flowing cold sodium. The dynamics of thermal striping were considered in computing values of film coefficient in the interface region even though thermal striping itself was neglected.

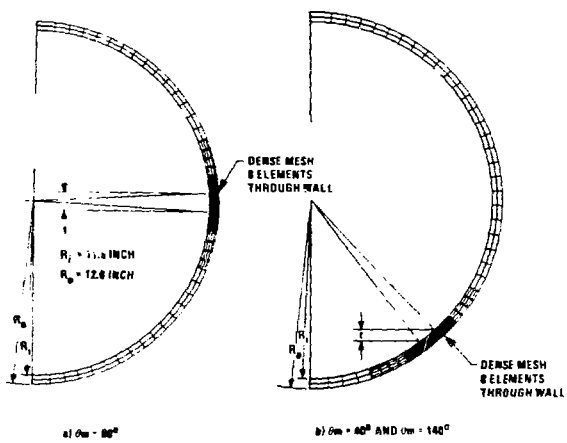


Figure 5 Finite Element Models of Static Stratified Flow

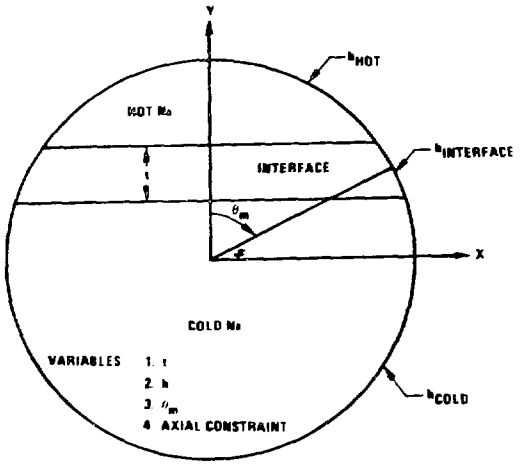


Figure 6 Definition of Variables for Parametric Study of Static Stratified Flow

Fujimoto concluded that film coefficients in the interface region can be as high as 7 times the nominal value. In this study the highest film coefficients were 10 times the nominal.

The location of the interface was varied from $\theta_m$ = 40° to $\theta_m$ = 140°. Extreme values of $\theta_m$ were not analyzed because they represent limiting cases which can be assessed in a simplified manner. At the initiation of a very low velocity event $\theta_m$ = 180° and $\theta_m$ approaches 0° at the end of an event. Stresses for these limiting values of $\theta_m$ can be readily analyzed by considering the entire pipe section as being isothermal with a local deviation in wall temperature equal to the maximum fluid $\Delta T$. In such cases, the region where the temperature differs can be assumed to be fully constrained by the remainder of the pipe. It is the intermediate values of $\theta_m$ which produce problems that are statically indeterminant and hence are of interest. The most prototypic axial constraint of the pipe is generalized plane strain with rotation. This constraint allows both a constant axial deflection and a constant rotation of the pipe cross section, i.e., the net axial force and net axial moment are zero. This corresponds to the commonly employed beam mode of deformation where plane sections remain plane. Generalized plane strain without rotation, i.e., $\varepsilon_{axial}$ = constant, is slightly over constraining. Plane strain i.e., $\varepsilon_{axial}$ = 0, is extremely over constraining and unrealistic and is not considered in this study.

The mechanics of the formation of stratification stresses provides insight to the structural response. Temperatures in the pipe were found to be nearly constant through the wall and were isothermal a short distance a short distance from the interface. The largest component of stress is axial which develops from differential axial expansion through the pipe cross section. The axial stresses are nearly constant through the pipe wall and therefore are appropriately termed "membrane". The distribution of axial stress around the circumference is a function of the axial constraint. The formation

**TABLE 2**

**VARIABLES IN PARAMETRIC STUDY OF STATIC STATE FLOW STRATIFICATION**

1. Interface Thickness

   - ○ t = 0"
   - ● t = 0.72"
   - ● t = 1.2"
   - ● t = 3.5"

2. Film Coefficient ($\frac{Btu}{Hr\text{-}Ft^2\text{-}°F}$)

   - ● High Values: $h_{HOT}$ = 900, $h_{INTERFACE}$ = 12000, $h_{COLD}$ = 1200
   - ● Low Values: $h_{HOT}$ = 450, $h_{INTERFACE}$ = 3000, $h_{COLD}$ = 600

   ● Prototypic Values

| $\theta_m$ | h HOT | h INTERFACE | h COLD |
|---|---|---|---|
| 40° | 900 | 9000 | 900 |
| 140° | 900 | 52000 | 5200 |

3. Location of Interface

   - ● High θ = 40°
   - ● Central θ = 90°
   - ● Low θ = 140°

4. Axial Constraint

   - ● Generalized plane strain w/rotation
   - ● Generalized plane strain w/o rotation

5. Temperature Difference

   - ● Hot Sodium = 1000°F
   - ● Cold Sodium = 600°F

of axial stresses and sample results are plotted in Figure 7 for the axial constraint of generalized plane strain with rotation. Hoop stresses develop due to differential radial expansion as illustrated in Figure 8. The hoop stresses are "bending" in nature and arises from the enforcement of compatability of the pipe in the interface region. It should also be noted in the example in Figure 8 that the maximum and minimum hoop stresses occur at the top and bottom of the pipe cross section and are small in magnitude compared to peak axial stresses. Radial stresses are small and are limited to maximum values of internal pressure in the pipe. Typical primary system pressures in LMFBRs are limited to several hundred psi. For the purpose of this assessment, radial stress is considered negligible.

Results from the parametric study are provided in Table 3. Only one parameter was varied in a given set of analyses. The most significant result is that the stress range and peak axial stress are not highly sensitive to relatively wide variations in interface thickness, film coefficient, location of the interface and axial constraint. The most pronounced variations occured due to changes in the interface thickness and axial constraint. The maximum elastic stress as well as the stress range decrease with the increasing interface thickness. Maximum stress and stress range for t=3.5 inches are 17 percent lower than those for t=0. Interface thicknesses observed in the water tests ranged from 0.6 inch to 2.0 inches while the interface thicknesses in actual sodium systems are expected to be larger based on the effect of Prandtl number.

The data in Table 3 show a 16 percent increase in stress when the cross section is constrained from rotating. The generalized plane strain with rotation

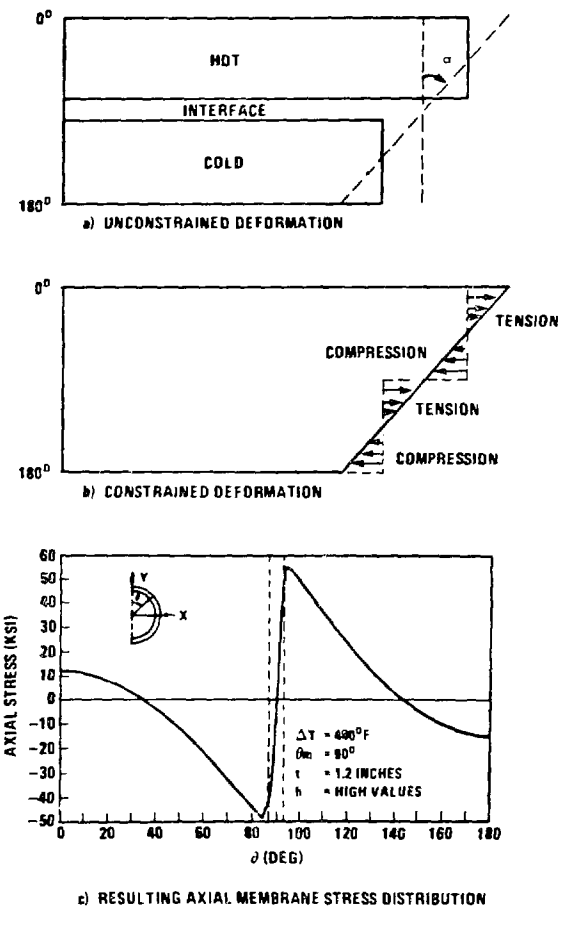


Figure 7 Formation of Axial Stress Due to Static Stratified Flow

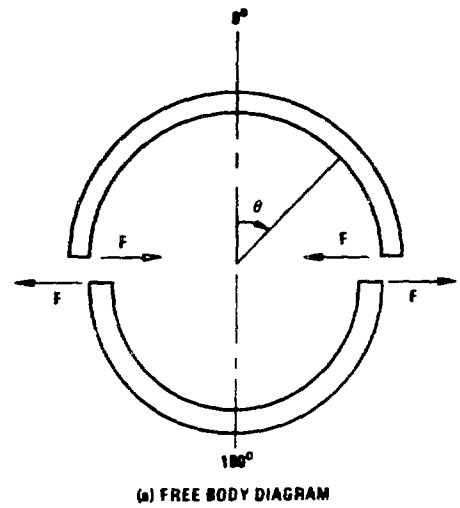


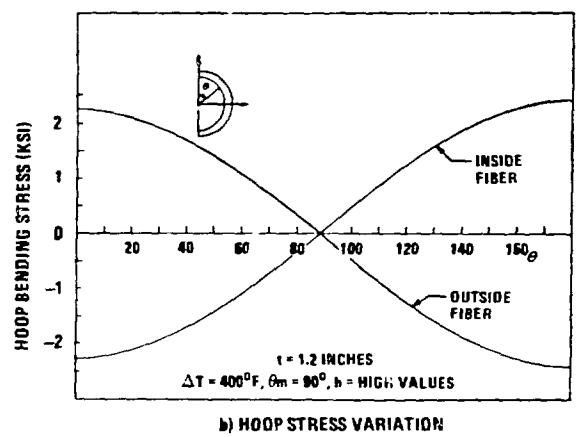


Figure 8 Formation of Hoop Stress Due to Static Stratified Flow

is however the most realistic and the rotation produced by stratification corresponds to a 3.3 degree rotation of the cross section over a 20 foot length of pipe. The maximum deflection of a pipe under these conditions would be 1.8 inches at the midpoint.

Results in Table 3 indicate that the stress range is minimum at $\theta_m = 90°$, but varies only 8 percent over a wide range of $\theta_m$. The axial stress components increase as $\theta_m$ decreases. However, for $40° < \theta_m < 140°$, the maximum stress varies by only 13 percent.

These results provide an interesting perspective on the widely used formula

$$\sigma_{max} = \frac{E\alpha\Delta T}{2} \qquad (2)$$

Eq. 2 represents the maximum stress resulting from full restraint of thermal bending. For this reason it provides a good approximation for the stress in a pipe in generalized plane strain without rotation. Since the rotation due to stratification is small, it also provides a good approximation for stress due to stratification. Eq. 2, evaluated for $\Delta T = 400°F$ using average material properties for 316 SS, yields a maximum stress of 53,000 psi. This is slightly higher than the maximum stress for $\theta_m = 40°$. The strain range is equal to twice this value, i.e., 106,000 psi, which is within 1 percent of the range predicted for generalized plane strain with constrained rotation. The upper limit of the elastic axial stress for the bounding cases of $\theta_m = 0°$ and $\theta_m = 180°$ will approach this value assuming the local region where the temperature differs is completely constrained by the remainder of the pipe. Finally, the variation is stress due to variations in film coefficient is insignificant being less than 5 percent.

Thermal Striping

Oscillation of the interface produces temperatures and stresses in the wall which are significantly different from the distributions resulting from a static interface. Through-the-wall variations in temperature and stress are highly nonlinear and time dependent. The frequency of oscillation was empirically determined to be in the range of 0.1 to 0.5 Hertz. Amplitudes up to 60 percent of the maximum fluid temperature difference were observed in the tests. The resulting temperature and stress distributions are analyzed here based on the assumption that curvature in the pipe wall can be neglected. For thermal distributions in a pipe wall the effect of radius is not important unless $R \sim 1/\sqrt{\omega/2\alpha}$. For $\omega = 0.5$ Hertz, $1/\sqrt{\omega/2\alpha} = 0.066$ inch which supports this assumption. Also the ratio R/b is 24 which makes this assumption valid for the structural response as well.

TABLE 3

STRESS RESULTS OF PARAMETRIC STUDY FOR

STATIC FLOW STRATIFICATION

1. Variation in t

| t (in.) | h | $\theta_m$ | Axial Constraint | Axial Stresses (psi) Maximum | Minimum | Range |
|---|---|---|---|---|---|---|
| 0 | HIGH* | 90° | GPS with Rotation | +48,100 | -43,000 | 91,100 |
| 0.72 | HIGH | 90° | GPS with Rotation | +48,000 | -42,800 | 90,800 |
| 1.2 | HIGH | 90° | GPS with Rotation | +47,200 | -42,000 | 89,200 |
| 3.5 | HIGH | 90° | GPS with Rotation | +41,000 | -37,000 | 78,000 |

2. Variation in h

| h | t (in) | $\theta_m$ | Axial Constraint | Axial Stresses (psi) Maximum | Minimum | Range |
|---|---|---|---|---|---|---|
| HIGH | 1.2 | 90° | GPS with Rotation | +47,200 | -42,000 | 89,200 |
| LOW | 1.2 | 90° | GPS with Rotation | +45,100 | -40,700 | 85,800 |

3. Variation in $\theta_m$

| $\theta_m$ | t (in) | h | Axial Constraint | Axial Stresses (psi) Maximum | Minimum | Range |
|---|---|---|---|---|---|---|
| 40° | 0.77 | HIGH | GPS with Rotation | +52,300 | -46,100 | 98,400 |
| 90° | 0.72 | HIGH | GPS with Rotation | +48,000 | -42,800 | 90,800 |
| 140° | 0.77 | HIGH | GPS with Rotation | +46,300 | -50,400 | 96,700 |
| 40° | 0.77 | PROTOTYPE | GPS with Rotation | +51,600 | -45,900 | 97,500 |
| 140° | 0.77 | PROTOTYPE | GPS with Rotation | +47,400 | -51,000 | 98,400 |

*See Table 2 for numerical values

Therefore, striping on a flat plate will adequately approximate thermal striping on the inside pipe wall. A sinusoidal variation in fluid temperature is assumed which is realistic based on the shape of temperature variations measured in the tests. (The sinusoidal wave shape is not apparent in Figure 3 due to the compression of the time scale).

The two principal variables which effect thermal striping stress are film coefficient and striping frequency. The attenuation of the amplitude of the fluid temperature fluctuation varies significantly over the range of frequency and film coefficient which are prototypic of stratified sodium. The attenuation of fluid temperature fluctuation through the fluid boundary layer is given by Jakob [3] as

$$\eta = \frac{1}{\sqrt{1+2(B/b^2) + 2(B/b^2)^2}} \qquad (3)$$

Table 4 provides values of $\eta$ for representative frequencies and film coefficients. $\eta$ is a strong function of film coefficient and is effected by frequency at lower values of film coefficient. Fujimoto observed that the values of dynamic film coefficients due to oscillations is stratified flow vary from 1.25 to 7 times the nominal value. Assuming that these factors can be applied to sodium, for the worst case conditions in this study the dynamic film coefficient would exceed 30,000 BTU/FT$^2$-Hr-°F and $\eta$ would approach unity. In order to insure conservatism, the attenuation of the thermal fluctuation through the fluid boundary is neglected. If the dynamic film coefficients are close to nominal values of h then $\eta$<<1 and the effect of thermal striping would be greatly reduced. The uncertainity in this assumption remains and additional research is needed to quantify dynamic effects in sodium.

The state of stress in the pipe is also dependent on frequency. The stress state due to thermal striping is biaxial and the state of strain is triaxial. The axial and hoop components of strain may be represented by

$$\epsilon_{axial} = \epsilon_{hoop} = \alpha(T - T_{average}) \qquad (4)$$

TABLE 4

ATTENUATION OF TEMPERATURE AMPLITUDE THROUGH FLUID BOUNDARY LAYER

| Frequency $\omega$ (Hertz) | Film Coefficient h BTU/Hr-Ft$^2$-°F | $\eta = \frac{\Delta T_{surface}}{\Delta T_{fluid}}$ |
|---|---|---|
| 0.5 | 1,000 | 0.27 |
| 0.5 | 15,000 | 0.87 |
| 0.5 | 30,000 | 0.93 |
| 0.1 | 1,000 | 0.47 |
| 0.1 | 15,000 | 0.94 |
| 0.1 | 30,000 | 0.97 |

where T represents the temperature at the point of strain and $T_{average}$ is the average temperature through the pipe wall. The radial strain is non-zero and is due to the Poisson's effect. Neglecting pressure, the radial stress is zero. The hoop and axial stress components can be readily derived from Hooke's law as

$$\sigma_{axial} = \sigma_{hoop} = \frac{E\alpha}{1-\nu}(T - T_{average}) \qquad (5)$$

In order to evaluate Eqs. 4 and 5 the transient temperature distributions must be known. Carslaw and Jaeger [4] provide a classical solution for a flat plate subject to harmonic variation in fluid temperature. Poindexter [5] gives an indepth examination of this solution with specific insight into the effects frequency and plate thickness. The maximum values of stress in Eq. 5 are given by Poindexter as

$$\sigma_{max} = \frac{E\alpha}{1-\nu}\left(\frac{\Delta T}{2}\right)\delta_{max} \qquad (6)$$

where $\Delta T$ represents the maximum range of surface temperature and

$$\delta = \left(\frac{T_{surface} - T_{average}}{\Delta T/2}\right) \qquad (7)$$

Poindexter also notes that

$$\delta = \phi(B) \qquad (8)$$

where $B = \sqrt{\omega/2\alpha}\,b$. $\delta$ approaches unity for large B. Hence the maximum surface stress occurs on a semi-infinite body. The same stress will develop for finite thickness if $\omega$ is sufficiently large. The examination of $\delta$ for prototypic frequencies and wall thickness indicates that the pipe wall resembles a thermally thick plate. Results given by Poindexter show that for $\omega$ = 0.5 Hertz and b = 0.5 inches, B = 3.37 and $\delta$ = 0.88. Thus the largest surface stress would occur at $\omega$ = 0.5 Hertz. For $\Delta T$ = 240°F Eq. 6 yields $\sigma_{max}$ = 42,600 psi. It is interesting to note that $\sigma_{max}$ is of the same order of magnitude as the maximum stress due to static stratification.

FATIGUE

Fatigue damage due to a static stratified interface and thermal striping are evaluated and compared in order to understand fatigue damage due to stratified flow. Fatigue design curves from the ASME Boiler and Pressure Vessel Code Case N-47 [7] are used as a basis of comparison. The effective strain range used in the fatigue calculations is defined as

$$\Delta\epsilon_t = \frac{\sqrt{2}}{2(1+\nu)}\left[(\Delta\epsilon_{radial} - \Delta\epsilon_{hoop})^2 + (\Delta\epsilon_{hoop} - \Delta\epsilon_{axial})^2 + (\Delta\epsilon_{axial} - \Delta\epsilon_{radial})^2\right]^{1/2} \qquad (9)$$

The state of stress through a pipe wall subject to static stratification is uniaxial and strain controlled. Hence, the effective strain range represented by Eq. 9 simplifies to

$$\Delta\epsilon_t^{\text{static stratification}} = \alpha\Delta T \qquad (10)$$

TABLE 5

SUMMARY OF WORST CASE FATIGUE DAMAGE

(T/C4 @ Location 2, 4.5 GPM)

| | n | ΔT (°F) | $\Delta\varepsilon^{*}_{t}$ (%) | $N_d$ | $\frac{n}{Nd}$ |
|---|---|---|---|---|---|
| Static Stratification | 1 | 400 | 0.44 | 936 | 0.00107 |
| Thermal Striping: | | | | | |
| Minimum ΔT | 15 | 40 | 0.0827 | $1.6\times10^{6}$ | $9\times10^{-6}$ |
| Average ΔT | 71 | 140 | 0.290 | 3630 | 0.0195 |
| Maximum ΔT | 16 | 240 | 0.496 | 712 | 0.0225 |
| | | | | $\Sigma\frac{n}{Nd}$ | 0.0431 |

*$\Delta\varepsilon_t = \alpha\Delta T$ for static stratification

$\Delta\varepsilon_t = \frac{\alpha\Delta T}{1-\nu}\delta_{max}$ for thermal striping

$\alpha = 11.0\times10^{-6}$ in/in-°F, $\delta_{max} = 0.94$, $\nu = 0.5$

The state of stress due to thermal striping is biaxial and Eqs. 4, 7 and 9 may be combined to give

$$\Delta\varepsilon_t \text{ thermal striping} = \frac{\alpha\Delta T}{1-\nu}\delta_{max} \qquad (11)$$

It should be noted that Eq. 11 is valid for elastic strain if $\nu = 0.3$ and plastic strain if $\nu = 0.5$. A value of $\nu = 0.5$ is used in this analysis to account for plastic strain.

In this assessment of fatigue damage, the inside pipe wall is assumed to encounter 1 strain cycle due to static stratification and the sum of the thermal striping cycles measured in the tests. Temperature fluctuations were converted to strain ranges via Eq. 11 and strain cycles were conservatively summed into three strain range groups. Total fatigue damage was calculated for each set of measurements using the 1000°-1200°F 316 SS fatigue design curve of Figure T-1420 in Reference 6. The worst total fatigue damage due to thermal striping occured at thermocouple 4 of location 2 for the 4.5 GPM flow rate. (This is the same data displayed in Figure 4.) A summary of the fatigue damage calculation is given in Table 5 along with the fatigue damage due to 1 cycle of static stratified flow.

Results in Table 5 clearly indicate that the fatigue damage from thermal striping is large relative to the fatigue damage due to static stratification. Less than 3 percent of the fatigue damage can be attributed to static stratified flow. Furthermore, the total damage due to 1 event is low. However, in a plant life there may be multiple duty cycle events which produce reverse flow and stratification may have the potential to produce significant fatigue damage and should therefore be considered in the analysis of piping designs. It is noted that the fatigue damages presented here are conservative. Actual thermal gradients in sodium piping systems will be less than those measured in the water tests due to the difference between the Prandlt numbers of water and sodium. Futhermore, worst case film coefficients were assumed in this analysis. More detailed cycle counting and less conservative estimates of plastic strain would also reduce the calculated fatigue damage.

## CONCLUSIONS

Stratified flow due to low velocity reverse flows has the potential to produce significant fatigue damage in primary pipe systems of loop type LMFBRs. In simulated water model tests the interface between the hot and cold stratified fluids was observed to oscillate in a wave motion producing thermal striping on the inside pipe wall. Thermal striping was identified as the major source of fatigue damage and it is most severe at low values of Richardson number.

The major uncertainties in this study are related to fluid behavior. Thermal gradients measured in water model tests are conservative due to the relative Prandtl numbers of water and sodium. However, the degree of conservatism has not been quantified and better correlation of water-to-sodium test date is needed. Also, high values of film coefficient were necessarily chosen to insure conversatism in the analysis of thermal striping. Current data show a wide variation in dynamic film coefficients. Fatigue due to thermal striping could be significantly reduced if lower values of film coefficient could be justified.

## ACKNOWLEDGEMENTS

This paper is based on work performed for the U.S. Department of Energy under contract No. DE-AC15-76CL050003. The author wishes to express his appreciation to Dr. R. H. Mallett for his support of this study and to Messrs. J. C. Reese and S. E. McIlvaine who designed and performed the water model tests.

## REFERENCES

1. Fujimoto, T., Sawada, K., Uregami, K., "Experimental Study of Striping at the Interface of Thermal Stratification," Thermal Hydraulics in Nuclear Technology, Ed. K. H. Sun, et. al., pp. 73-78, American Society of Mechanical Engineers, New York, 1981.

2. Filstrup, A. W., "WECAN: Westinghouse Electric Computer Analysis. A General Finite Element Program for Structural Analysis, "Westinghouse Research Laboratories, Pittsburgh, PA, 1973.

3. Jakob, M., Heat Transfer, Vol. 1, J. Wiley, New York, 1949.

4. Carslaw, H. S. and Jaeger, J. C., Conduction of Heat on Solids, Oxford University Press, New York, 1947.

5. Poindexter, A. M., "Thermal Response of a Flat Plate of Finite Thickness Immersed in a Fluid with Oscillating Temperature," Nuclear Technology, 55, pp. 656-661 (1981).

6. ASME Boiler and Pressure Vessel Code, "Case N-47, Class 1 Components in Elevated Temperature Service, Section III, Division 1," American Society of Mechanical Engineers, New York, 1977.

Refer to:
WR830608

Westinghouse Electric Corporation
Advanced Power Systems Divisions

Waltz Mill Site
Box 158
Madison Pennsylvania 15663

September 15, 1983

U. S. Department of Energy
Technical Information Center
P. O. Box 62
Oak Ridge, TN 37830

Subject: Clinch River Breeder Reactor Plant; Release of Technical Paper under Contract DE-AC15-76CL50003

Dear Sir:

Enclosed are two (2) copies of the technical paper entitled "Fatigue of LMFBR Piping Due to Flow Stratification" by W. S. Woodward.

The paper has been patent cleared by the U.S. DOE Oak Ridge Patent Office and approved by the CRBRP Project Office for release to TIC. It was presented at the ASME Pressure Vessel and Piping Conference in Portland, Oregon in June 1983 and published in the proceedings thereof.

This letter satisfies commitment number LR6287.

Very truly yours,

W. R. Hull, Manager
CRBRP Contracts

/pjc
Enclosures

CM-83-1175

cc: w/Enclosure - DOE/OR - Chief, Information Division, C. Sandoz (2)
- W-OR - O. A. Nelson
w/o Enclosure - W-OR - Project Manager, W. J. Purcell

Form DOE-426
(1/79)

**U.S. DEPARTMENT OF ENERGY**

**DOE AND MAJOR CONTRACTOR RECOMMENDATIONS FOR DISPOSITION OF SCIENTIFIC AND TECHNICAL DOCUMENT**

*See Instructions on Reverse Side*

| 1. DOE Report No. | 2. Contract No. | 3. Subject Category No. |
|---|---|---|
| | DE-AC15-76CL50003 | |

4. Title
Fatigue of LMFBR Piping Due to Flow Stratification

5. Type of Document ("x" one)
- ☐ a. *Scientific and technical report*
- ☒ b. Conference paper: Title of conference ASME Pressure Vessel and Piping Conference
  Date of conference June 1983
  Exact location of conference Portland, OR Sponsoring organization ASME
- ☐ c. Other (Specify Thesis, Translations, etc.)

6. Copies Transmitted ("x" one or more)
- ☐ a. Copies being transmitted for standard distribution by DOE-TIC.
- ☐ b. Copies being transmitted for special distribution per attached complete address list.
- ☒ c. Two completely legible, reproducible copies being transmitted to DOE-TIC.
- ☐ d. Twenty seven copies being transmitted to DOE-TIC for TIC processing and NTIS sales.

7. Recommended Distribution ("x" one)
- ☒ a. Normal handling (after patent clearance): no restraints on distribution except as may be required by the security classification.

Make available only ☐ b to U.S. Government agencies and their contractors. ☐ c. within DOE and to DOE contractors.
☐ d. within DOE. ☐ e. to those listed in item 13 below.

- ☐ f. Other (Specify)

8. Recommended Announcement ("x" one)
- ☒ a. *Normal procedure may be followed.* ☐ b. Recommend the following announcement limitations:

9. Reason for Restrictions Recommended in 7 or 8 above.
- ☐ a. Preliminary information. ☐ b. Prepared primarily for internal use. ☐ c. Other (Explain)

N/A

10. Patent Clearance
Does this information product disclose any new equipment, process or material? ☐ Yes ☒ No
Has an invention disclosure been submitted to DOE covering any aspect of this information product? If so, identify the DOE (or other) disclosure number and to whom the disclosure was submitted. ☐ Yes ☒ No

Are there any patent related objections to the release of this information product? If so, state these objections.

("x" one)
- ☒ a. DOE patent clearance has been granted by responsible DOE patent group.
- ☐ b. Document has been sent to responsible DOE patent group for clearance.

11. National Security Information (For classified document only; "x" one)
Document ☐ a. does ☐ b. does not contain national security information other than restricted data.

12. Copy Reproduction and Distribution
Total number of copies reproduced _____ Number of copies distributed outside originating organization _____

13. Additional Information or Remarks (Continue on separate sheet, if necessary)
Contains Applied Technology

14. Submitted by (Name and Position) (Please print or type)
W. R. Hull, Manager, CPBRP Contracts

Organization
Westinghouse Electric Corp., Advanced Energy Systems Div., Madison, PA 15663

Signature _____ Date 9/14/83

# FATIGUE OF LMFBR PIPING DUE TO FLOW STRATIFICATION

W. S. WOODWARD
Senior Engineer
Member ASME
Westinghouse Electric Corp.
Madison, PA

## ABSTRACT

Flow stratification due to reverse flow was simulated in a 1/5 scale water model of a LMFBR primary pipe loop. The stratified flow was observed to have a dynamic interface region which oscillated in a wave pattern. The behavior of the interface was characterized in terms of location, local temperature fluctuation and duration for various reverse flow conditions. A structural assessment was performed to determine the effects of stratified flow on the fatigue life of the pipe. Both the static and dynamic aspects of flow stratification were examined. The dynamic interface produces thermal striping on the inside of the pipe wall which is shown to have the most deleterious effect on the pipe wall and produce significant fatigue damage relative to a static interface.

## INTRODUCTION

Flow stratification is a phenomenon which has the potential to cause significant fatigue damage in liquid metal pipe systems. Stratified flow can occur in loop type LMFBR primary pipe systems during remote events which involve both a pony motor failure in one loop and check valve leakage. During these events reverse flow may initiate in the affected loop and cold sodium residing in the intermediate heat exchanger (IHX) is pushed backwards out of the inlet nozzle and up through the hot leg pipe. Flow stratification may develop when the cold sodium reaches a horizontal pipe section containing hot sodium. The controlling parameter for identifying the initation of flow stratification is the dimensionless Richardson number. The Richardson number represents the ratio of bouyancy forces to the inertial forces in the fluid flow. The bouyancy forces are due to the difference in density between the hot and cold fluids and under low velocity reverse flow conditions the bouyancy forces dominate the inertial forces and stratification develops. The interface region between the hot and cold sodium layers is of particular interest because large variations in local fluid temperature coupled with characteristically high film coefficients can produce large variations in temperature in the pipe wall. The resulting thermal stress fluctuations contribute to fatigue of the pipe.

Until recently there has been little research directed toward the understanding of flow stratification in piping systems. The fluid phenomenon is currently being evaluated by Kasza at Argonne National Laboratory for piping systems prototypic of those found in loop type LMFBRs. This test program is intended to give pipe designers an understanding of the problem and provide recommendations on how to minimize stratification

## NOMENCLATURE

| | |
|---|---|
| $b$ | Thickness of pipe wall |
| $D$ | Inside diameter of a pipe |
| $D_h$ | Hydraulic diameter = 4·(Flow area)/(Wetted perimeter) |
| $E$ | Young's modulus |
| $g$ | Gravitation acceleration |
| $h$ | Film coefficient |
| $k$ | Thermal conductivity |
| $R_i$ | Inside radius of pipe |
| $R_o$ | Outside radius of pipe |
| $t$ | Thickness of interface region |
| $V$ | Flow velocity |
| $\alpha$ | Thermal diffusivity |
| $\beta$ | Dimensionless thickness, $\sqrt{w/2ab}$ |
| $\varepsilon$ | Strain |
| $\Delta\rho$ | Difference in density due to temperature difference $\Delta T$ |
| $\Delta T$ | Maximum temperature difference in fluid |
| $\delta$ | Surface to average temperature difference |
| $\eta$ | $\Delta T$ surface/$\Delta T$ fluid |
| $\theta_m$ | Angle from vertical indicating location of central position of the stratified interface |
| $\rho$ | Density |
| $\omega$ | Frequency of oscillation |

effects. Kasza has developed a correlation between the Richardson number and the initiation of flow stratification. These results indicate that stratification will probably develop during low velocity reverse flow events in LMFBR primary pipe systems. Fujimoto [1] performed tests to investigate flow stratification in pipes with the specific purpose of studying the fluid behavior in the vicinity of the interface between the hot and cold fluids. He observed significant wave motion at the interface which resembled the wave motion of flow in an open channel. Moreover, he concluded that the film coefficients at the interface were as high as seven times nominal values. Although these studies provide key data in quantifying the fluid phenomenon, they do not address the effects of stratification on the pipe structure.

The purpose of the present study is to provide an understanding of how flow stratification contributes to fatigue damage in LMFBR primary pipe systems. Stratified flow was simulated for reverse flow conditions in a series of scaled water tests. The fluid behavior was observed and local fluid temperature fluctuations were measured. Under reverse flow conditions, highly dynamic thermal fluctuations were observed which were due to the wave motions of the interface of the hot and cold fluid layers. In this study, fatigue damage due to static stratified flow and the dynamic wave motions are examined. It is demonstrated that the dynamic nature of stratification can be the most deleterious to the pipe wall.

## WATER MODEL TESTS

Reverse flow events, typical of those which occur in loop type LMFBR primary pipe systems, were simulated in scaled water model tests. The objective is to obtain fluid temperatures for use in calculating pipe wall temperatures and subsequently thermal stresses and fatigue damage. The model was constructed from plexiglass pipe and is illustrated in Figure 1. The model includes a large diameter (6.5 inch I.D.) hot leg which connects the reactor vessel with the primary pump and a smaller diameter (4.0 inch I.D.) hot leg connecting the primary pump and intermediate heat exchanger (IHX). The volume of fluid in the pump model is representative of the volume of fluid in a scaled primary pump, however, the pump dynamics were not modeled. The pipe model was initially filled with static 130°F water. Reverse flow was simulated by injecting 70°F water at the IHX inlet. Dye was injected into the cold stream for flow visualization. Transient fluid temperature were measured at cross sections 1 through 5 (Figure 1) using closely spaced thermocouples around the circumference of the pipe wall. The thermocouples were Type K grounded thermocouples with time constants in a range of 0.1 - 0.3 seconds. Figure 2 illustrates the placement of thermocouples in the cross sections. This arrangement was designed specifically to detect the location of the interface between the hot and cold layers as stratified flow developes and moves up through the cross section.

### Test Conditions

The selection of parameters for the scaled water tests was based on similitude of the Richardson number

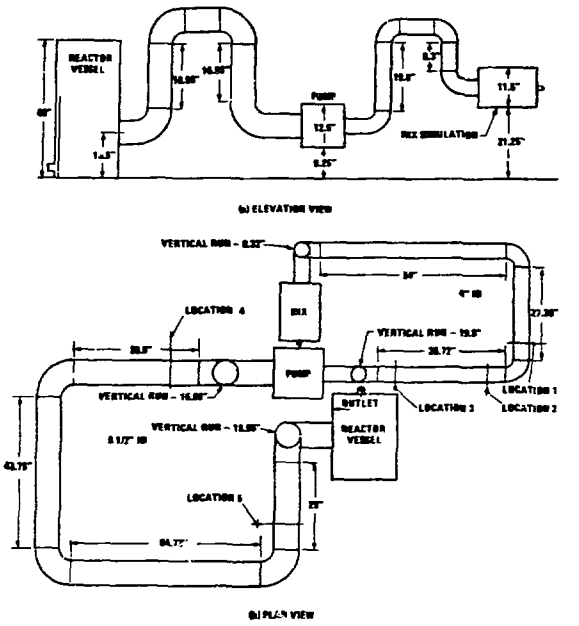


Figure 1 Water Model of a LMFBR Primary Hot Leg

$$Ri = \frac{\Delta\rho}{\rho}\,\frac{gD}{v^2} \qquad (1)$$

Reverse flow velocities were selected such that Richardson numbers in the tests were equal to prototypic values for a LMFBR primary pipe system. Maximum reverse flows in current LMFBR designs are limited by check valve leakage to 1100 GPM. The maximum difference in sodium temperature for reverse flow events in loop type LMFBRs is 400°F. Diameters of 23 inches and 35 inches were used as diameters for prototypic hot leg pipes and Richardson numbers were calculated for maximum reverse flow velocities in each pipe leg. Test flow rates were based on simulation of 42 percent to 100 percent of the maximum reverse flow rates. The selected test conditions are summarized in Table 1.

Establishing similitude based on the Richardson number does not insure complete similitude between the model and prototype. The Reynolds numbers should be equivalent for dynamic similitude and the Prandtl numbers should be equivalent for thermal similitude. For these tests similitude of both the Reynolds number and Prandtl number cannot be established concurrently with the similitude of the Richardson number. The Reynolds numbers of the reverse flow for actual plant events are turbulent being in a range of $10^5$-$10^6$. The Reynolds numbers in the tests fall in the laminar to turbulent transition range (Table 1). Thus, the dynamics of the fluid in the test do not simulate that of the plant. Although similitude in dynamics is not rigoriously established, tests which have turbulent flow regimes should provide reasonable dynamic simulation. Moreover, the thermal

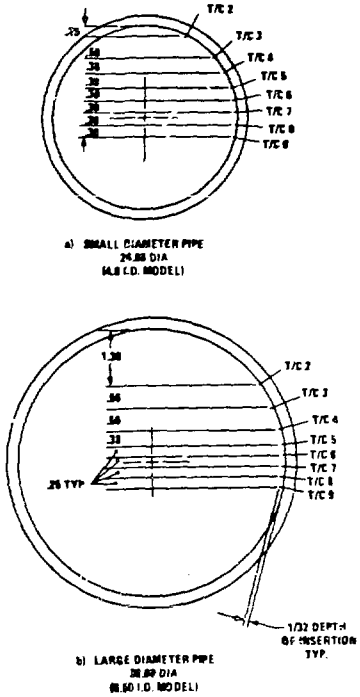


Figure 2 Location of Thermocouples in Pipe Cross Sections

gradients in actual plant events are expected to be much lower than in the tests because the Prandtl number of sodium is of the order of 1000 times lower than that of water. The effect of Prandtl number is judged to dominate over any differences in dynamic behavior between the test and the plant. Thus, thermal gradients observed in the water tests will be greater than those in a LMFBR primary pipe system and thermal stresses calculated from the water test data will be conservative.

## Observations and Results

Stratification was observed to develop under all test conditions. The interface between the hot and cold fluids moved slowly up through the cross sections until the entire pipe was filled with cold fluid. Based on the duration and the amplitude of fluid temperature difference, the worst locations in the small and large pipe sections were 2 and 5 respectively. Figure 3 illustrates the temperature distribution at location 2. The time required to completely wash out the hot fluid increased with increasing Richardson number. Illustrating this point, stratification disappeared after 500 seconds at location 2 for a flow rate of 6.0 GPM while it persisted after 4000 seconds at location 5 with a flow rate of 3.0 GPM. The thickness of the interface region, within which the temperature changed from the hot fluid temperature to that of the cold fluid, varied in the range of 0.6 to 2 inches.

TABLE 1

SUMMARY OF TEST CONDITIONS

| Pipe Section | Cold Water Flow Rate (GPM) | Ri | Re* $\times 10^3$ |
|---|---|---|---|
| 4.0 inch I.D. | 6.0 | 5.3 | 8.5 |
| | 4.5 | 9.5 | 6.4 |
| | 3.0 | 21.4 | 4.3 |
| 6.5 inch I.D. | 7.1 | 44.0 | 6.1 |
| | 5.0 | 88.0 | 4.3 |
| | 3.0 | 244 | 2.3 |

* $Re = \frac{VD_h}{\nu}$. V and $D_h$ are based on reverse flow through bottom half of pipe.

Another significant observation was the oscillation of the interface region. Forces in the shear flow caused the stratified interface to fluctuate in a wave motion similar to that described by Fujimoto. This was most pronounced at low Richardson numbers. The movement of the interface region causes severe transient thermal fluctuations in the pipe wall termed "thermal striping". Figure 4 illustrates the resulting local temperature variation for the worst case thermal striping. Note that the curves in Figure 3 denote average data because local fluctuations such as those shown in Figure 4, are filtered out. The frequency of the thermal striping varies between 0.1 and 0.5 Hertz and under worst case conditions the amplitudes are as high as 60 percent of the maximum difference in fluid temperature. The worst case thermal striping was measured by thermocouple 4 at location 2 during the 4.5 GPM test. The duration of the striping was 440 seconds. A total of 102 cycles was counted. Fifteen percent of this total measured less than ten percent of the fluid $\Delta T$. Seventy percent of the cycles were less than thirty-five percent of the fluid $\Delta T$ while only two percent measured less than sixty percent of the fluid $\Delta T$. Thus only a small percent of the total cycles approached the maximum amplitude.

Thus, two sources of fatigue were identified in these tests. The first source is from stress due to the presence of a static stratified fluid which maintains the top of the pipe at a higher temperature than the bottom. The second source is from stress due to the dynamics of the interface region which produces thermal striping on the pipe wall. The thermal stresses which result from these two phenomena are examined in the next section.

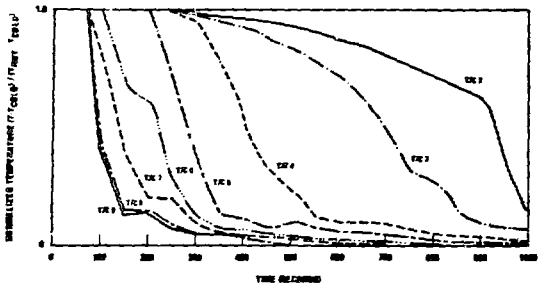

Figure 3 Worst Case Average Temperature Distributions in the Small Diameter Pipe

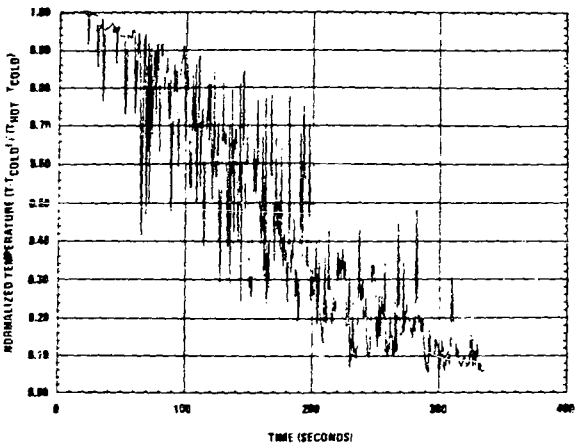


Figure 4 Response of Thermocouple Illustrating Worst Case Thermal Striping Fluctuations

## THERMAL STRESSES

Thermal stresses which result from stratification were studied as a basis for assessing fatigue damage. In order to simplify the analysis, the thermal gradients in the pipe wall were decoupled into two categories based on the two features of stratification previously identified. They are:

A. static stratification represented by hot and cold layers of sodium separated by an interface region and

B. thermal striping due to the oscillation of the interface.

Neglecting oscillation of the interface, the movement of the stratification up through the pipe cross section is sufficiently slow that the assumption of the "static" interface closely approximates the phenomenon. The thermal and stress distributions for this problem are essentially time independent. In contrast, the oscillation of the interface is relatively fast, producing time-dependent distributions of temperature and stress in the pipe wall. The distributions of temperature and elastic stress for both of these problems are examined in this section.

### Static Flow Stratification

The temperature gradients and stresses due to static stratified flow were assessed using the WECAN finite element program [2]. Finite element models were constructed of 2-D quadratic isoparametric elements and are illustrated in Figure 5. The models represent a large diameter thin walled 316 SS pipe, typical of those found in loop type LMFBRs. The fluid was modeled as an isothermal hot (1000°F) layer of sodium residing over an isothermal cold (600°F) layer of sodium separated by an interface region within which the fluid temperature varied linearly. A parametric study was performed to examine the sensitivity of solutions to variables which are necessarily assumed in the analysis. The parameters varied in the thermal analysis are the interface thickness, t, the film coefficients in each region, h, and the location of the interface $\theta_m$. These variables are illustrated in Figure 6. Linear elastic stress solutions were generated from the resulting thermal distributions and the additional variable of pipe constraint was introduced in the calculation of stress. Internal pressure was neglected.

The values of the variables examined in the parametric study are listed in Table 2. Interface thicknesses span those observed in the water model test. The largest value was judged to be representative of actual in sodium gradients. The heat transfer between the fluid and pipe was modeled while the outside pipe was adiabatic. Bounding values of film coefficients were based on static hot sodium and flowing cold sodium. The dynamics of thermal striping were considered in computing values of film coefficient in the interface region even though thermal striping itself was neglected.

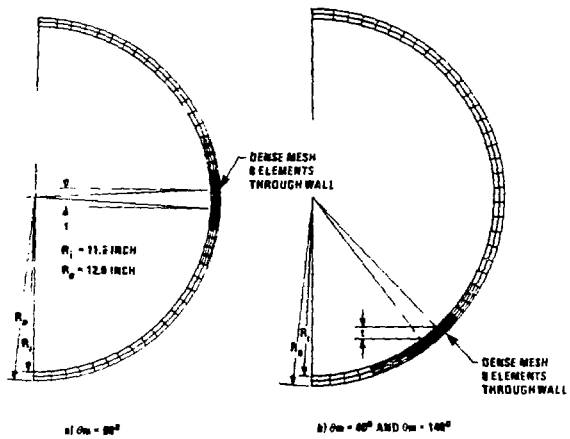


Figure 5 Finite Element Models of Static Stratified Flow

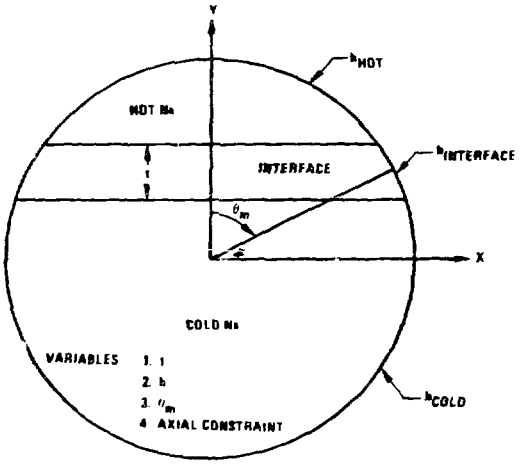


Figure 6 *Definition of Variables for Parametric Study of Static Stratified Flow*

Fujimoto concluded that film coefficients in the interface region can be as high as 7 times the nominal value. In this study the highest film coefficients were 10 times the nominal.

The location of the interface was varied from $\theta_m = 40°$ to $\theta_m = 140°$. Extreme values of $\theta_m$ were not analyzed because they represent limiting cases which can be assessed in a simplified manner. At the initiation of a very low velocity event $\theta_m = 180°$ and $\theta_m$ approaches 0° at the end of an event. Stresses for these limiting values of $\theta_m$ can be readily analyzed by considering the entire pipe section as being isothermal with a local deviation in wall temperature equal to the maximum fluid $\Delta T$. In such cases, the region where the temperature differs can be assumed to be fully constrained by the remainder of the pipe. It is the intermediate values of $\theta_m$ which produce problems that are statically indeterminant and hence are of interest. The most prototypic axial constraint of the pipe is generalized plane strain with rotation. This constraint allows both a constant axial deflection and a constant rotation of the pipe cross section, i.e., the net axial force and net axial moment are zero. This corresponds to the commonly employed beam mode of deformation where plane sections remain plane. Generalized plane strain without rotation, i.e., $\epsilon_{axial}$ = constant, is slightly over constraining. Plane strain i.e., $\epsilon_{axial} = 0$, is extremely over constraining and unrealistic and is not considered in this study.

The mechanics of the formation of stratification stresses provides insight to the structural response. Temperatures in the pipe were found to be nearly constant through the wall and were isothermal a short distance a short distance from the interface. The largest component of stress is axial which develops from differential axial expansion through the pipe cross section. The axial stresses are nearly constant through the pipe wall and therefore are appropriately termed "membrane". The distribution of axial stress around the circumference is a function of the axial constraint. The formation

TABLE 2

VARIABLES IN PARAMETRIC STUDY OF STATIC STATE FLOW STRATIFICATION

1. Interface Thickness

- t = 0"
- t = 0.72"
- t = 1.2"
- t = 3.5"

2. Film Coefficient ($\frac{Btu}{Hr\text{-}Ft^2\text{-}°F}$)

- High Values: $h_{HOT} = 900$, $h_{INTERFACE} = 12000$, $h_{COLD} = 1200$
- Low Values: $h_{HOT} = 450$, $h_{INTERFACE} = 3000$, $h_{COLD} = 600$
- Prototypic Values:

| $\theta_m$ | $h_{HOT}$ | $h_{INTERFACE}$ | $h_{COLD}$ |
|---|---|---|---|
| 40° | 900 | 9000 | 900 |
| 140° | 900 | 52000 | 5200 |

3. Location of Interface

- High $\theta = 40°$
- Central $\theta = 90°$
- Low $\theta = 140°$

4. Axial Constraint

- Generalized plane strain w/rotation
- Generalized plane strain w/o rotation

5. Temperature Difference

- Hot Sodium = 1000°F
- Cold Sodium = 600°F

of axial stresses and sample results are plotted in Figure 7 for the axial constraint of generalized plane strain with rotation. Hoop stresses develop due to differential radial expansion as illustrated in Figure 8. The hoop stresses are "bending" in nature and arises from the enforcement of compatability of the pipe in the interface region. It should also be noted in the example in Figure 8 that the maximum and minimum hoop stresses occur at the top and bottom of the pipe cross section and are small in magnitude compared to peak axial stresses. Radial stresses are small and are limited to maximum values of internal pressure in the pipe. Typical primary system pressures in LMFBRs are limited to several hundred psi. For the purpose of this assessment, radial stress is considered negligible.

Results from the parametric study are provided in Table 3. Only one parameter was varied in a given set of analyses. The most significant result is that the stress range and peak axial stress are not highly sensitive to relatively wide variations in interface thickness, film coefficient, location of the interface and axial constraint. The most pronounced variations occured due to changes in the interface thickness and axial constraint. The maximum elastic stress as well as the stress range decrease with the increasing interface thickness. Maximum stress and stress range for t=3.5 inches are 17 percent lower than those for t=0. Interface thicknesses observed in the water tests ranged from 0.6 inch to 2.0 inches while the interface thicknesses in actual sodium systems are expected to be larger based on the effect of Prandtl number.

The data in Table 3 show a 16 percent increase in stress when the cross section is constrained from rotating. The generalized plane strain with rotation

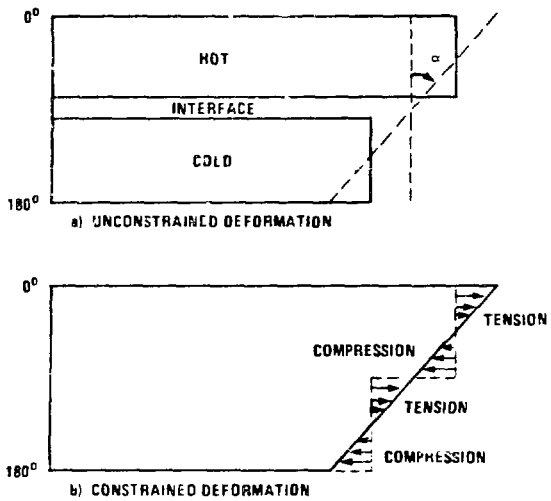


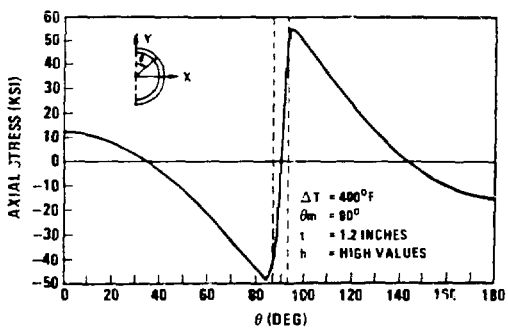


c) RESULTING AXIAL MEMBRANE STRESS DISTRIBUTION

Figure 7 Formation of Axial Stress Due to Static Stratified Flow

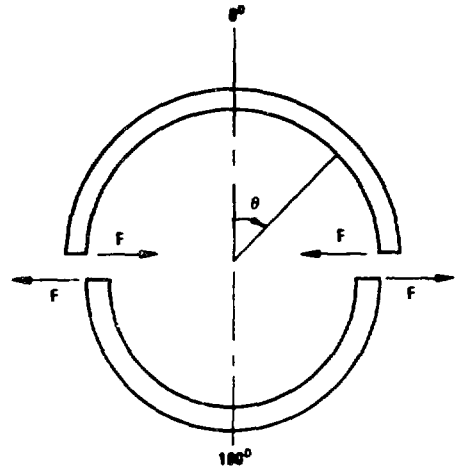


(a) FREE BODY DIAGRAM

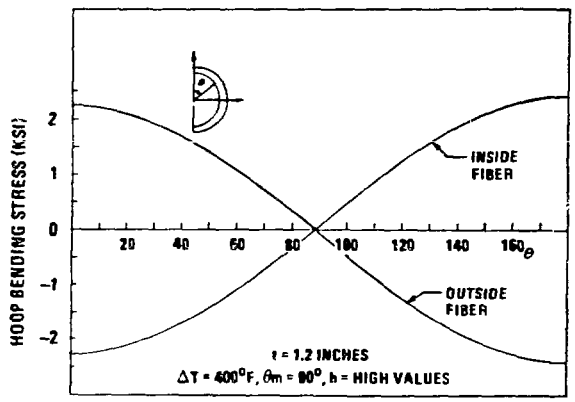


b) HOOP STRESS VARIATION

Figure 8 Formation of Hoop Stress Due to Static Stratified Flow

is however the most realistic and the rotation produced by stratification corresponds to a 3.3 degree rotation of the cross section over a 20 foot length of pipe. The maximum deflection of a pipe under these conditions would be 1.8 inches at the midpoint.

Results in Table 3 indicate that the stress range is minimum at $\theta_m = 90°$, but varies only 8 percent over a wide range of $\theta_m$. The axial stress components increase as $\theta_m$ decreases. However, for $40° < \theta_m < 140°$, the maximum stress varies by only 13 percent.

These results provide an interesting perspective on the widely used formula

$$\sigma_{max} = \frac{E\alpha\Delta T}{2} \qquad (2)$$

Eq. 2 represents the maximum stress resulting from full restraint of thermal bending. For this reason it provides a good approximation for the stress in a pipe in generalized plane strain without rotation. Since the rotation due to stratification is small, it also provides a good approximation for stress due to stratification. Eq. 2, evaluated for $\Delta T = 400°F$ using average material properties for 316 SS, yields a maximum stress of 53,000 psi. This is slightly higher than the maximum stress for $\theta_m = 40°$. The strain range is equal to twice this value, i.e., 106,000 psi, which is within 1 percent of the range predicted for generalized plane strain with constrained rotation. The upper limit of the elastic axial stress for the bounding cases of $\theta_m = 0°$ and $\theta_m = 180°$ will approach this value assuming the local region where the temperature differs is completely constrained by the remainder of the pipe. Finally, the variation in stress due to variations in film coefficient is insignificant being less than 5 percent.

Thermal Striping

Oscillation of the interface produces temperatures and stresses in the wall which are significantly different from the distributions resulting from a static interface. Through-the-wall variations in temperature and stress are highly nonlinear and time dependent. The frequency of oscillation was empirically determined to be in the range of 0.1 to 0.5 Hertz. Amplitudes up to 60 percent of the maximum fluid temperature difference were observed in the tests. The resulting temperature and stress distributions are analyzed here based on the assumption that curvature in the pipe wall can be neglected. For thermal distributions in a pipe wall the effect of radius is not important unless $R \sim 1/\sqrt{\omega/2\alpha}$. For $\omega = 0.5$ Hertz, $1/\sqrt{\omega/2\alpha} = 0.066$ inch which supports this assumption. Also the ratio R/b is 24 which makes this assumption valid for the structural response as well.

TABLE 3

STRESS RESULTS OF PARAMETRIC STUDY FOR

STATIC FLOW STRATIFICATION

1. Variation in t

| t (in.) | h | $\theta_m$ | Axial Constraint | Axial Stresses (psi) Maximum | Minimum | Range |
|---|---|---|---|---|---|---|
| 0 | HIGH* | 90° | GPS with Rotation | +48,100 | -43,000 | 91,100 |
| 0.72 | HIGH | 90° | GPS with Rotation | +48,000 | -42,800 | 90,800 |
| 1.2 | HIGH | 90° | GPS with Rotation | +47,200 | -42,000 | 89,200 |
| 3.5 | HIGH | 90° | GPS with Rotation | +41,000 | -37,000 | 78,000 |

2. Variation in h

| h | t (in) | $\theta_m$ | Axial Constraint | Axial Stresses (psi) Maximum | Minimum | Range |
|---|---|---|---|---|---|---|
| HIGH | 1.2 | 90° | GPS with Rotation | +47,200 | -42,000 | 89,200 |
| LOW | 1.2 | 90° | GPS with Rotation | +45,100 | -40,700 | 85,800 |

3. Variation in $\theta_m$

| $\theta_m$ | t (in) | h | Axial Constraint | Axial Stresses (psi) Maximum | Minimum | Range |
|---|---|---|---|---|---|---|
| 40° | 0.77 | HIGH | GPS with Rotation | +52,300 | -46,100 | 98,400 |
| 90° | 0.72 | HIGH | GPS with Rotation | +48,000 | -42,800 | 90,800 |
| 140° | 0.77 | HIGH | GPS with Rotation | +46,300 | -50,400 | 96,700 |
| 40° | 0.77 | PROTOTYPE | GPS with Rotation | +51,600 | -45,900 | 97,500 |
| 140° | 0.77 | PROTOTYPE | GPS with Rotation | +47,400 | -51,000 | 98,400 |

*See Table 2 for numerical values

Therefore, striping on a flat plate will adequately approximate thermal striping on the inside pipe wall. A sinusoidal variation in fluid temperature is assumed which is realistic based on the shape of temperature variations measured in the tests. (The sinusoidal wave shape is not apparent in Figure 3 due to the compression of the time scale).

The two principal variables which effect thermal striping stress are film coefficient and striping frequency. The attenuation of the amplitude of the fluid temperature fluctuation varies significantly over the range of frequency and film coefficient which are prototypic of stratified sodium. The attenuation of fluid temperature fluctuation through the fluid boundary layer is given by Jakob [3] as

$$\eta = \frac{1}{\sqrt{1+2(B/b^2) + 2(B/b^2)^2}} \qquad (3)$$

Table 4 provides values of $\eta$ for representative frequencies and film coefficients. $\eta$ is a strong function of film coefficient and is effected by frequency at lower values of film coefficient. Fujimoto observed that the values of dynamic film coefficients due to oscillations is stratified flow vary from 1.25 to 7 times the nominal value. Assuming that these factors can be applied to sodium, for the worst case conditions in this study the dynamic film coefficient would exceed 30,000 BTU/Ft$^2$-Hr-°F and $\eta$ would approach unity. In order to insure conservatism, the attenuation of the thermal fluctuation through the fluid boundary is neglected. If the dynamic film coefficients are close to nominal values of h then $\eta$<<1 and the effect of thermal striping would be greatly reduced. The uncertainity in this assumption remains and additional research is needed to quantify dynamic effects in sodium.

The state of stress in the pipe is also dependent on frequency. The stress state due to thermal striping is biaxial and the state of strain is triaxial. The axial and hoop components of strain may be represented by

$$\varepsilon_{axial} = \varepsilon_{hoop} = \alpha(T - T_{average}) \qquad (4)$$

TABLE 4

ATTENUATION OF TEMPERATURE AMPLITUDE THROUGH FLUID BOUNDARY LAYER

| Frequency $\omega$ (Hertz) | Film Coefficient h BTU/Hr-Ft$^2$-°F | $\eta = \frac{\Delta T \text{ surface}}{\Delta T \text{ fluid}}$ |
|---|---|---|
| 0.5 | 1,000 | 0.27 |
| 0.5 | 15,000 | 0.87 |
| 0.5 | 30,000 | 0.93 |
| 0.1 | 1,000 | 0.47 |
| 0.1 | 15,000 | 0.94 |
| 0.1 | 30,000 | 0.97 |

where T represents the temperature at the point of strain and $T_{average}$ is the average temperature through the pipe wall. The radial strain is non-zero and is due to the Poisson's effect. Neglecting pressure, the radial stress is zero. The hoop and axial stress components can be readily derived from Hooke's law as

$$\sigma_{axial} = \sigma_{hoop} = \frac{E\alpha}{1-\nu}(T - T_{average}) \qquad (5)$$

In order to evaluate Eqs. 4 and 5 the transient temperature distributions must be known. Carslaw and Jaeger [4] provide a classical solution for a flat plate subject to harmonic variation in fluid temperature. Poindexter [5] gives an indepth examination of this solution with specific insight into the effects frequency and plate thickness. The maximum values of stress in Eq. 5 are given by Poindexter as

$$\sigma_{max} = \frac{E\alpha}{1-\nu}\left(\frac{\Delta T}{2}\right)\delta_{max} \qquad (6)$$

where $\Delta T$ represents the maximum range of surface temperature and

$$\delta = \left(\frac{T_{surface} - T_{average}}{\Delta T/2}\right) \qquad (7)$$

Poindexter also notes that

$$\delta = \phi(B) \qquad (8)$$

where $B = \sqrt{\omega/2\alpha}\,t$. $\delta$ approaches unity for large B. Hence the maximum surface stress occurs on a semi-infinite body. The same stress will develop for finite thickness if $\omega$ is sufficiently large. The examination of $\delta$ for prototypic frequencies and wall thickness indicates that the pipe wall resembles a thermally thick plate. Results given by Poindexter show that for $\omega$ = 0.5 Hertz and b = 0.5 inches, B = 3.37 and $\delta$ = 0.88. Thus the largest surface stress would occur at $\omega$ = 0.5 Hertz. For $\Delta T$ = 240°F Eq. 6 yields $\sigma_{max}$ = 42,600 psi. It is interesting to note that $\sigma_{max}$ is of the same order of magnitude as the maximum stress due to static stratification.

FATIGUE

Fatigue damage due to a static stratified interface and thermal striping are evaluated and compared in order to understand fatigue damage due to stratified flow. Fatigue design curves from the ASME Boiler and Pressure Vessel Code Case N-47 [7] are used as a basis of comparison. The effective strain range used in the fatigue calculations is defined as

$$\Delta\varepsilon_t = \frac{\sqrt{2}}{2(1+\nu)}\left[\Delta\varepsilon_{radial} - \Delta\varepsilon_{hoop}\right)^2 + \left(\Delta\varepsilon_{hoop} - \Delta\varepsilon_{axial}\right)^2 + \left(\Delta\varepsilon_{axial} - \Delta\varepsilon_{radial}\right)^2\Big]^{1/2} \qquad (9)$$

The state of stress through a pipe wall subject to static stratification is uniaxial and strain controlled. Hence, the effective strain range represented by Eq. 9 simplifies to

$$\Delta\varepsilon_t^{\text{static stratification}} = \alpha\Delta T \qquad (10)$$

TABLE 5

SUMMARY OF WORST CASE FATIGUE DAMAGE

(T/C4 @ Location 2, 4.5 GPM)

| | n | ΔT (°F) | $\Delta\varepsilon^*_t$ (%) | $N_d$ | $\frac{n}{N_d}$ |
|---|---|---|---|---|---|
| Static Stratification | 1 | 400 | 0.44 | 936 | 0.00107 |
| Thermal Striping: | | | | | |
| Minimum ΔT | 15 | 40 | 0.0827 | $1.6\times10^{6}$ | $9\times10^{-6}$ |
| Average ΔT | 71 | 140 | 0.290 | 3630 | 0.0195 |
| Maximum ΔT | 16 | 240 | 0.496 | 712 | 0.0225 |
| | | | | $\Sigma\frac{n}{N_d}$ | 0.0431 |

*$\Delta\varepsilon_t = \alpha\Delta T$ for static stratification

$\Delta\varepsilon_t = \frac{\alpha\Delta T}{1-\upsilon}\delta_{max}$ for thermal striping

$\alpha = 11.0\times10^{-6}$ in/in-°F, $\delta_{max} = 0.94$, $\upsilon = 0.5$

The state of stress due to thermal striping is biaxial and Eqs. 4, 7 and 9 may be combined to give

$$\Delta\varepsilon_{t\ \text{thermal striping}} = \frac{\alpha\Delta T}{1-\upsilon}\delta_{max} \qquad (11)$$

It should be noted that Eq. 11 is valid for elastic strain if $\upsilon = 0.3$ and plastic strain if $\upsilon = 0.5$. A value of $\upsilon = 0.5$ is used in this analysis to account for plastic strain.

In this assessment of fatigue damage, the inside pipe wall is assumed to encounter 1 strain cycle due to static stratification and the sum of the thermal striping cycles measured in the tests. Temperature fluctuations were converted to strain ranges via Eq. 11 and strain cycles were conservatively summed into three strain range groups. Total fatigue damage was calculated for each set of measurements using the 1000°-1200°F 316 SS fatigue design curve of Figure T-1420 in Reference 6. The worst total fatigue damage due to thermal striping occured at thermocouple 4 of location 2 for the 4.5 GPM flow rate. (This is the same data displayed in Figure 4.) A summary of the fatigue damage calculation is given in Table 5 along with the fatigue damage due to 1 cycle of static stratified flow.

Results in Table 5 clearly indicate that the fatigue damage from thermal striping is large relative to the fatigue damage due to static stratification. Less than 3 percent of the fatigue damage can be attributed to static stratified flow. Furthermore, the total damage due to 1 event is low. However, in a plant life there may be multiple duty cycle events which produce reverse flow and stratification may have the potential to produce significant fatigue damage and should therefore be considered in the analysis of piping designs. It is noted that the fatigue damages presented here are conservative. Actual thermal gradients in sodium piping systems will be less than those measured in the water tests due to the difference between the Prandlt numbers of water and sodium. Futhermore, worst case film coefficients were assumed in this analysis. More detailed cycle counting and less conservative estimates of plastic strain would also reduce the calculated fatigue damage.

## CONCLUSIONS

Stratified flow due to low velocity reverse flows has the potential to produce significant fatigue damage in primary pipe systems of loop type LMFBRs. In simulated water model tests the interface between the hot and cold stratified fluids was observed to oscillate in a wave motion producing thermal striping on the inside pipe wall. Thermal striping was identified as the major source of fatigue damage and it is most severe at low values of Richardson number.

The major uncertainties in this study are related to fluid behavior. Thermal gradients measured in water model tests are conservative due to the relative Prandtl numbers of water and sodium. However, the degree of conservatism has not been quantified and better correlation of water-to-sodium test data is needed. Also, high values of film coefficient were necessarily chosen to insure conservatism in the analysis of thermal striping. Current data show a wide variation in dynamic film coefficients. Fatigue due to thermal striping could be significantly reduced if lower values of film coefficient could be justified.

## ACKNOWLEDGEMENTS

This paper is based on work performed for the U.S. Department of Energy under contract No. DE-AC15-76CL050003. The author wishes to express his appreciation to Dr. R. H. Mallett for his support of this study and to Messrs. J. C. Roese and S. E. McIlvaine who designed and performed the water model tests.

## REFERENCES

1. Fujimoto, T., Sawada, K., Uragami, K., "Experimental Study of Striping at the Interface of Thermal Stratification," Thermal Hydraulics in Nuclear Technology, Ed. K. H. Sun, et. al., pp. 73-78, American Society of Mechanical Engineers, New York, 1981.

2. Filstrup, A. W., "WECAN: Westinghouse Electric Computer Analysis. A General Finite Element Program for Structural Analysis, "Westinghouse Research Laboratories, Pittsburgh, PA, 1973.

3. Jakob, M., Heat Transfer, Vol. 1, J. Wiley, New York, 1949.

4. Carslaw, H. S. and Jaeger, J. C., Conduction of Heat on Solids, Oxford University Press, New York, 1947.

5. Poindexter, A. M., "Thermal Response of a Flat Plate of Finite Thickness Immersed in a Fluid with Oscillating Temperature," Nuclear Technology, 55, pp. 656-661 (1981).

6. ASME Boiler and Pressure Vessel Code, "Case N-47, Class 1 Components in Elevated Temperature Service, Section III, Division 1," American Society of Mechanical Engineers, New York, 1977.